Highly stable loading of Mcm proteins onto chromatin in living cells requires replication to unload

Marjorie A. Kuipers,[1] Timothy J. Stasevich,[2] Takayo Sasaki,[1] Korey A. Wilson,[1] Kristin L. Hazelwood,[3] James G. McNally,[2] Michael W. Davidson,[3] and David M. Gilbert[1]

[1]Department of Biological Science, Florida State University, Tallahassee, FL 32306
[2]Laboratory of Receptor Biology and Gene Expression, National Cancer Institute, National Institutes of Health, Bethesda, MD 20892
[3]National High Magnetic Field Laboratory and Department of Biological Science, Florida State University, Tallahassee, FL 32310

The heterohexameric minichromosome maintenance protein complex (Mcm2-7) functions as the eukaryotic helicase during DNA replication. Mcm2-7 loads onto chromatin during early G1 phase but is not converted into an active helicase until much later during S phase. Hence, inactive Mcm complexes are presumed to remain stably bound from early G1 through the completion of S phase. Here, we investigated Mcm protein dynamics in live mammalian cells. We demonstrate that Mcm proteins are irreversibly loaded onto chromatin cumulatively throughout G1 phase, showing no detectable exchange with a gradually diminishing soluble pool. Eviction of Mcm requires replication; during replication arrest, Mcm proteins remained bound indefinitely. Moreover, the density of immobile Mcms is reduced together with chromatin decondensation within sites of active replication, which provides an explanation for the lack of colocalization of Mcm with replication fork proteins. These results provide in vivo evidence for an exceptionally stable lockdown mechanism to retain all loaded Mcm proteins on chromatin throughout prolonged cell cycles.

Introduction

The mechanisms ensuring complete duplication of the eukaryotic genome exactly once per cell cycle are highly conserved and coordinated by two mutually exclusive alternating periods of the cell cycle (Masai et al., 2010). First, during early G1 phase, Cdk activity is diminished because of the continuous destruction of cyclins by the anaphase-promoting complex (APC). Under these conditions, replication cannot initiate, but the origin recognition complex (ORC), along with Cdc6 and Cdt1, can load an inactive form of the Mcm2-7 hexameric helicase onto chromatin to form prereplication complexes (preRCs). Second, during late G1 phase, CDK and Dbf4-dependent Cdc7 kinase (DDK) activities rise and cooperate with a suite of other proteins to both prevent any further preRC assembly and initiate replication. Initiation of replication continues throughout S phase by converting the inactive "loaded" minichromosome maintenance protein complexes (Mcms) into active helicases (Wei et al., 2010) triggered by DDK (Bousset and Diffley, 1998; Donaldson et al., 1998; Pasero et al., 1999; Sheu and Stillman, 2010). Hence, unlike prokaryotic helicases that are activated soon after loading, eukaryotes temporally separate the loading and activation of the helicase. In addition to preventing rereplication, this temporal separation may allow eukaryotes to ensure that there are a sufficient number of Mcm complexes loaded to replicate large chromosomes in a timely fashion (Remus and Diffley, 2009). In fact, checkpoint mechanisms may prevent the entry into S phase until sufficient numbers of Mcms are loaded (Ge and Blow, 2009; Liu et al., 2009; Nevis et al., 2009).

The separation in time between the loaded and active forms of Mcm can be quite prolonged. In mammalian cells, for

M.A. Kuipers and T.J. Stasevich contributed equally to this paper.

Correspondence to David M. Gilbert: gilbert@bio.fsu.edu

Abbreviations used in this paper: BLT, biotin ligase tag; DDK, Dbf4-dependent Cdc7 kinase; dox, doxycycline; IF, immobile fraction; FLIP, fluorescence loss in photobleaching; mEm, monomeric Emerald; ODP, origin decision point; ORC, origin recognition complex; PCNA, proliferating cell nuclear antigen; preRC, prereplication complex; R point, restriction point; RFP, red fluorescent protein; tet, tetracycline.

The Rockefeller University Press $30.00
J. Cell Biol. Vol. 192 No. 1 29–41
www.jcb.org/cgi/doi/10.1083/jcb.201007111

those Mcm complexes destined to be activated near the end of a normal cell cycle, as well as any Mcms whose activation is delayed by checkpoint mechanisms, the separation can be days. With the exception of core histones (Manser et al., 1980; Kimura and Cook, 2001), and possibly cohesins (G2 phase residence time >6 h; Gerlich et al., 2006), no chromatin proteins have been demonstrated to remain associated this long, and even histones can be evicted from specific regions by remodeling or transcription (Deal et al., 2010). All other chromatin proteins examined have residence times of seconds to minutes (Phair et al., 2004; Mueller et al., 2010), including the preRC proteins ORC (McNairn et al., 2005) and Cdt1 (Xouri et al., 2007). The longest reported residence time for any replication protein is 10–20 min for the processivity factor proliferating cell nuclear antigen (PCNA; Essers et al., 2005).

Recently, it was shown that purified preRC proteins assemble Mcms as a closed double-hexameric ring around double-stranded DNA (Evrin et al., 2009; Remus et al., 2009), which predicts a highly stable topologically linked Mcm–DNA interaction. However, the existence of a double hexamer has yet to be demonstrated in living cells. In addition, two states of chromatin-associated Mcm have been distinguished biochemically by high-salt extraction (Edwards et al., 2002; Evrin et al., 2009; Francis et al., 2009; Remus et al., 2009; Rowles et al., 1999; Tsakraklides and Bell, 2010). Both states require ORC, Cdc6, and Cdt1 to assemble, but the high-salt resistant state requires the ATP-dependent dissociation of these other preRC components, and is the preferred substrate for DDK. These studies have led to a model whereby Mcm loading is a two-step process beginning with ATP-bound ORC and Cdc6 recruiting Mcm2-7-Cdt1 heptamers to form the associated complex, followed by ATP hydrolysis–driven loading of an Mcm2-7 double hexamer topologically linked to dsDNA and release of ORC, Cdc6, and Cdt1.

These in vitro findings raise several intriguing questions regarding the in vivo behavior of Mcm proteins. First, can one detect an unusually stable Mcm–chromatin interaction that can persist for an entire cell cycle? Second, can one distinguish an associated versus loaded complex based on in vivo residence times, and how long after association does Mcm loading occur? To date, experiments extracting Mcm proteins from cellular chromatin have not detected changes in Mcm binding during G1 phase, but important changes in the in vivo on/off rates of chromatin proteins are frequently not reflected in chromatin extraction assays (Mueller et al., 2010). Third, what fraction of associated Mcm complexes are loaded and have helicase potential? For example, there is evidence that some Mcm subunits perform nonreplicational roles (Ferguson and Maller, 2008) such as transcription (Zhang et al., 1998; Yankulov et al., 1999; DaFonseca et al., 2001; Snyder et al., 2005), and when performing such roles Mcm molecules may interact differently with chromatin. Moreover, Mcm2-7 proteins do not colocalize with sites of DNA synthesis or replication proteins that presumably share the replication fork with the active helicase (Todorov et al., 1995; Krude et al., 1996; Romanowski et al., 1996; Dimitrova et al., 1999). One explanation for this longstanding paradox is that the majority of Mcms exist in a more loosely associated form and become released during initiation, leaving behind a small number of helicase-competent Mcms that are difficult to detect by immunofluorescence (Dimitrova et al., 1999).

To address these questions, we performed quantitative live cell imaging of fluorescent Mcm proteins in CHO cells. We detected only two populations of Mcm molecules in the cell: an unbound population consistent with freely diffusing molecules and a completely immobile or bound population. Remarkably, we could not detect any exchange between these two pools of molecules. From G2 phase through mitosis, all Mcm molecules were in the unbound form. During G1 phase, the bound fraction of Mcm proteins increased gradually until the majority of Mcm proteins were bound just before S phase. After DNA synthesis began, Mcm proteins were gradually converted to an unbound form at a rate accounted for by the progression of S phase. Importantly, when DNA synthesis was arrested, the bound Mcm fraction remained immobile for >24 h. Our results provide in vivo evidence for a "lockdown, kickoff" mechanism in which Mcm2-7 complexes loaded during G1 phase remain irreversibly bound throughout the cell cycle until they are released by the act of replication. In addition, our results suggest that the lack of colocalization of Mcms with replication fork proteins is caused by the decondensation of chromatin and consequent dilution of Mcm proteins at sites of DNA synthesis.

Results

Establishment of a system for live cell cycle analysis of Mcm dynamics

We constructed C-terminal fusions of all six mouse Mcm subunits to monomeric Emerald (mEm), one of the brightest fluorescing variants of GFP (Fig. S1; Rothbauer et al., 2008). All fusions were also epitope-tagged at the C terminus of mEm with an optimized peptide substrate for the *Escherichia coli* biotin ligase (BirA) enzyme (Fig. 1 A) to facilitate efficient avidin affinity purification (Beckett et al., 1999; de Boer et al., 2003). Each Mcm-mEm was first transiently transfected into CHO cells to verify fluorescence and nuclear localization. Consistent with prior work (Kimura et al., 1996), Mcm2 and Mcm3 localized to the nucleus, whereas Mcm4-7 required cotransfection with either Mcm2 or Mcm3 to enter the nucleus (unpublished data). To construct stable cell lines that express Mcm-mEm at physiological levels, Mcm-mEms were expressed under the control of a tetracycline (tet)/doxycycline (dox)-regulatable promoter. This allows cell lines to be established under repressed conditions, followed by controlled induction before experimentation (Izumi and Gilbert, 1999; McNairn et al., 2005).

Each Mcm fusion construct was transfected into a CHO cell line stably expressing both the tet transactivator tTA and the BirA enzyme. Individual clonal cell lines were selected and expanded in the presence of dox, and aliquots of each cell line were passaged in the absence of dox to evaluate Mcm-mEm expression. Only stable cell lines in which all cells in the population expressed homogeneous, inducible levels of Mcm-mEm were selected for further characterization (Fig. 1 B). Mcm2- and Mcm3-mEm were exclusively nuclear independent of dox concentration, whereas Mcm4-7–mEm all had a cytoplasmic

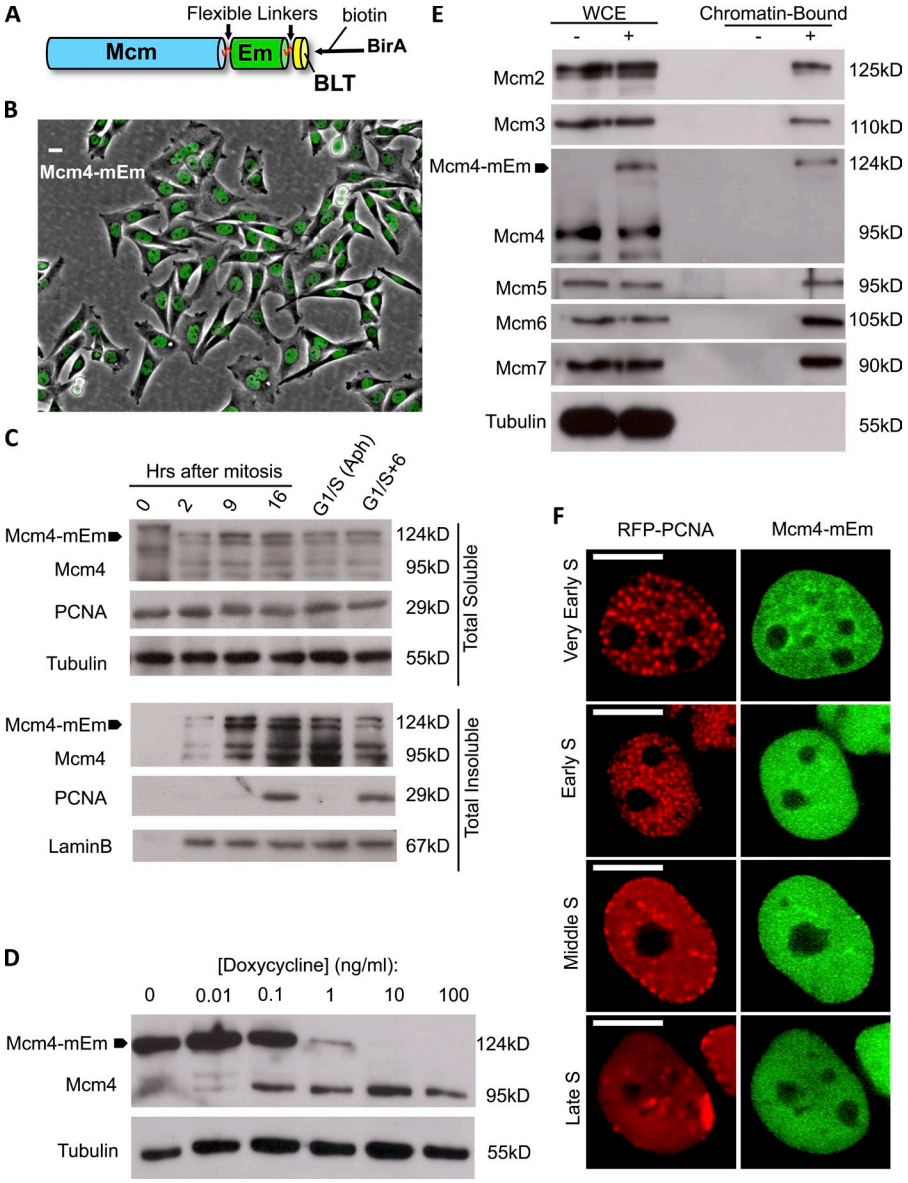

Figure 1. **Characterization of cell lines.** (A) Structure of Mcm-fluorescent protein (Mcm-mEm) fusion proteins. Each Mcm-mEm contains a full-length Mcm2-7 cDNA (Kimura et al., 1996), followed by a flexible linker, the fluorescent protein, a second flexible linker, and an optimized peptide substrate (BLT) for the *E. coli* biotin ligase enzyme (BirA). (B) Homogenous expression of Mcm4-mEm. After transfection of the expression cassette shown in A, cells were selected in the presence of dox to establish cell lines in the absence of Mcm-mEm expression. Dox was then removed from aliquots of each cell line for 48 h to induce tagged protein. Shown is Mcm4-mEm fluorescence merged with a phase contrast image. Bar, 10 µm. (C) Cell cycle regulation of soluble and insoluble fractions of endogenous and tagged Mcm4-mEm. Cells were synchronized in mitosis by shake-off and detergent-extracted at the indicated times after replating. Aliquots of cells were plated into aphidicolin for 16 h to arrest cells at the G1/S phase border (G1/S Aph), and a portion of those cells were released into S phase for 6 h (G1/S+6). The soluble and insoluble fractions (Fig. S4 A) were subjected to immunoblotting with the indicated antibodies. Both tagged and endogenous Mcm4 are completely soluble and exhibit a molecular weight shift during mitosis, as expected (Pereverzeva et al., 2000; Okuno et al., 2001). During G1, both tagged and endogenous Mcm4 present as a doublet band when sufficient care is taken to inhibit phosphatases, as expected (Komamura-Kohno et al., 2006). Insoluble PCNA tracks S phase; note that aphidicolin arrest results in increased detergent extractability of PCNA. β-Tubulin and LaminB are used as loading controls for the soluble and insoluble fractions, respectively. Both tagged and endogenous Mcm4 are reduced in the insoluble fraction 6 h after release from aphidicolin, as expected (Okuno et al., 2001). (D) Autogenous regulation of Mcm4-mEm. Mcm4-mEm–expressing cells were grown in the indicated concentrations of dox, and whole cell extracts were subjected to immunoblotting with an anti-Mcm4 antibody. Anti–β-tubulin was used as a loading control. (E) Coprecipitation of Mcm4-mEm with endogenous Mcm subunits in chromatin from late G1 phase cells. Cells either expressing (+) or not expressing (−) Mcm4-mEm were synchronized in mitosis and collected 8 h after release into G1 phase, and Mcm4-mEm (indicated with a black arrow) was precipitated from the solubilized chromatin fragments (Chromatin-Bound; Fig. S4 A). Whole cell extracts (WCE) from the same cells are also shown. Mcm4-mEm–expressing cells were grown in 0.5 ng/ml dox for 24 h before harvesting to eliminate all cytoplasmic Mcm4-mEm expression. Note that endogenous Mcm4 did not pull down with the tagged Mcm4, which indicates that double hexamers containing both tagged and untagged subunits are rare under these conditions, but this does not imply that they do not exist. Their abundance may depend on the ratio of tagged and untagged proteins bound to chromatin (e.g., see Fig. S4 C). (F) RFP-PCNA displays cell cycle–dependent punctate patterns in Mcm-mEm cell lines. Shown are cells in very early (initial appearance of PCNA foci), early, mid, or late S phase displaying the characteristic spatial patterns of PCNA (red) at sites of ongoing DNA synthesis. Note that Mcm4-mEm (green) is distributed heterogeneously in very early S phase but more homogeneously as S phase proceeds. PCNA is distributed uniformly in both G1 and G2 phase (Fig. 2, B and C). Bars, 10 µm.

component in the absence of dox but could be rendered exclusively nuclear by titrating the concentration of dox (unpublished data). These results, together with those from transient transfection (described in the previous paragraph), are consistent with chaperoning of Mcm4-7 proteins into the nucleus by endogenous Mcm2 or -3 (Kimura et al., 1996), the quantities of which become saturated at high Mcm4-7–mEm expression.

Next, we compared the intranuclear distribution of chromatin-bound and soluble Mcm-mEms to endogenous Mcms during the cell cycle. After extraction of soluble protein, Mcm-mEms were found to colocalize with endogenous Mcm2 early in the cell cycle (Fig. S2 A) and to clear off chromatin together in the appropriate cell cycle–regulated fashion during the progression of S phase (Fig. 1 C and Figs. S2 A). To determine the relative levels of expression of endogenous and exogenous Mcm proteins at various levels of dox, we performed Western blots of whole cell extracts from Mcm-mEm–expressing cells grown in the presence of varying levels of dox. Surprisingly, Mcm3-, Mcm4-, and Mcm7-mEm, but not Mcm6-mEm, displayed a marked reduction of the endogenous Mcm subunit in the absence of

dox (Fig. 1 D and Fig. S3, A and B). Thus, cells appear to stringently regulate the levels of at least some Mcm subunits such that when the tagged protein is induced, the amount of endogenous protein is reduced. This demonstrates that cells can survive with the tagged protein as their primary Mcm subunit, which provides compelling evidence for their functionality without the need to perform knockdown.

To confirm that Mcm-mEm fusion proteins interact with the other endogenous subunits of the Mcm2-7 complex, avidin coprecipitation experiments were performed with whole cell extracts of Mcm-mEm–expressing cells. Precipitated proteins were subjected to Western blotting with antibodies to endogenous Mcm2-7 proteins (Fig. S3, C–E). All Mcm-mEm except Mcm5-mEm were found to form complexes with endogenous subunits. For reasons we do not understand, Mcm5-mEm could pull down Mcm2 and -3 but not -4 or -7. In addition, Mcm5-mEm localized to centrosomes, as shown by others for transient transfections of epitope-tagged Mcm5 (Ferguson and Maller, 2008). Hence, we did not pursue further studies of Mcm5-mEm. To verify that the Mcm-mEm–containing complexes could load onto chromatin, detergent-extracted nuclei were digested with nuclease to release chromatin fragments (Méndez and Stillman, 2000), which were then precipitated with avidin beads to pull down Mcm-mEm. Results confirmed that Mcm-mEm formed complexes with endogenous subunits bound to chromatin during G1 phase (Fig. 1 E and Fig. S4).

To relate Mcm dynamics to the progression of cells through S phase, Mcm-mEm–expressing cell lines were further stably transfected with a red fluorescent protein (RFP)-tagged PCNA (Leonhardt et al., 2000). RFP-PCNA was homogenously distributed throughout the nucleus in non–S phase cells (Fig. 2, B and C), but during S phase, they displayed punctate spatial patterns of replication foci characteristic of very early, early, middle, or late S phase (Fig. 1 F), as previously characterized for endogenous PCNA by immunohistochemistry (O'Keefe et al., 1992; Dimitrova et al., 1999). RFP-PCNA colocalized with endogenous PCNA replication foci (Fig. S2 B) and did not interfere with the progression of cells through the cell cycle, as measured by flow cytometry (Fig. S2 D) or by long-term imaging of cells through the cell cycle (Videos 1 and 2). In contrast to PCNA, Mcm-mEm proteins were homogenously distributed throughout the nucleus at all cell cycle time points except during late G1 and very early S phase, when they displayed a heterogeneous pattern (Fig. 1 F) consistent with an accumulation of Mcm-mEm proteins on chromatin.

Cell cycle–regulated dynamics of Mcm4

We focused our initial studies on the Mcm4 subunit because of its presumed importance in activation by Cdc7 (Masai et al., 2006) and its interaction with the GINS complex (Ilves et al., 2010). To identify the position of individual cells in the cell cycle without the use of drug synchronization regimes that could alter preRC protein dynamics, we devised the protocols shown in Fig. 2 (and Videos 3 and 4). Cells in early G1 phase (Fig. 2 A) were identified by first marking cells undergoing mitosis and then returning to those cells at various time points thereafter. For the purposes of these experiments, the onset of G1 phase was defined as the time at which Mcm-mEm entered the nucleus (between 5 and 10 min in Fig. 2 A and at 2 s in Video 3). Cells were then bleached at times between 1 and 5 h after the onset of G1 phase (S phase began 7–12 h after mitosis). Cells in late G1 were identified by their homogeneous PCNA and heterogeneous Mcm fluorescence, whereas cells in early G1 or G2 showed homogenous fluorescence for both proteins. The time from the photobleaching until the first appearance of PCNA foci (30–60 min in Fig. 2 B and at 26 min in Video 4) further verified their precise position in late G1. Cells in different stages of S phase were identified by the spatial pattern of PCNA foci (Fig. 1 F). Finally, cells in G2 phase were identified by marking cells with late S phase PCNA spatial patterns and photobleaching those cells after the completion of S phase, as indicated by the absence of PCNA foci (135 min after cell identification in Fig. 2 C).

Using these protocols, we performed FRAP experiments on cells expressing Mcm4-mEm at various stages of the cell cycle. Representative FRAP recovery curves are shown in Fig. 3. Recoveries immediately after entry of Mcm in the nucleus were rapid and complete, lasting <1 min, whereas FRAP recoveries in G1 revealed an immobile fraction (IF) that lasted many hours. In early G1, the IF was ∼34%, and steadily increased during progression through G1. After the onset of S phase, as determined by the appearance of PCNA foci, no further loading of Mcm4 was observed. Instead, cells exhibited a slow and gradual FRAP recovery that coincided very closely with the initial appearance of PCNA foci (Fig. 3, gray bars). In mid to late S-phase cells, the IF decreased from <10% to barely detectable in late S and G2 phase (Fig. 3 and Video 5). Together, these results suggest that Mcm4 is loaded gradually throughout G1 phase and unloaded throughout S phase, which is consistent with prior studies with fixed cells (Todorov et al., 1995; Dimitrova et al., 1999).

Loaded Mcm4 does not exchange and requires replication to unload

Surprisingly, the results in Fig. 3 did not conform to any of our existing models for steady-state chromatin protein exchange (Mueller et al., 2010; Stasevich et al., 2010). Instead, they were most closely fit to a model in which bound Mcm4 does not exchange at all with the soluble pool. We reasoned that the FRAP recovery observed after S phase begins could arise exclusively from an increased soluble pool of unbleached molecules as they are evicted during replication. To test this hypothesis, we took several approaches. In the first approach, a series of short FRAP experiments (<1 min each) were conducted to measure the IF at various time points after the entry into S phase. As shown in Fig. 4 A, the IF of Mcm4 was found to decay as S phase progressed, and this decay could be fit with a single linear or weak exponential function that yielded a decay time of ∼13.5 h, approximately the length of S phase. Next, we identified 10 cells in which long FRAP experiments (>150 min each) were initiated in late G1, ∼100 min before the beginning of S phase. If Mcm4 is not exchanging, FRAP recoveries should equal the IF decay time and reflect the unloading of unbleached molecules that subsequently diffuse freely throughout the nucleus. However, if Mcm4 is exchanging, then FRAP recoveries should

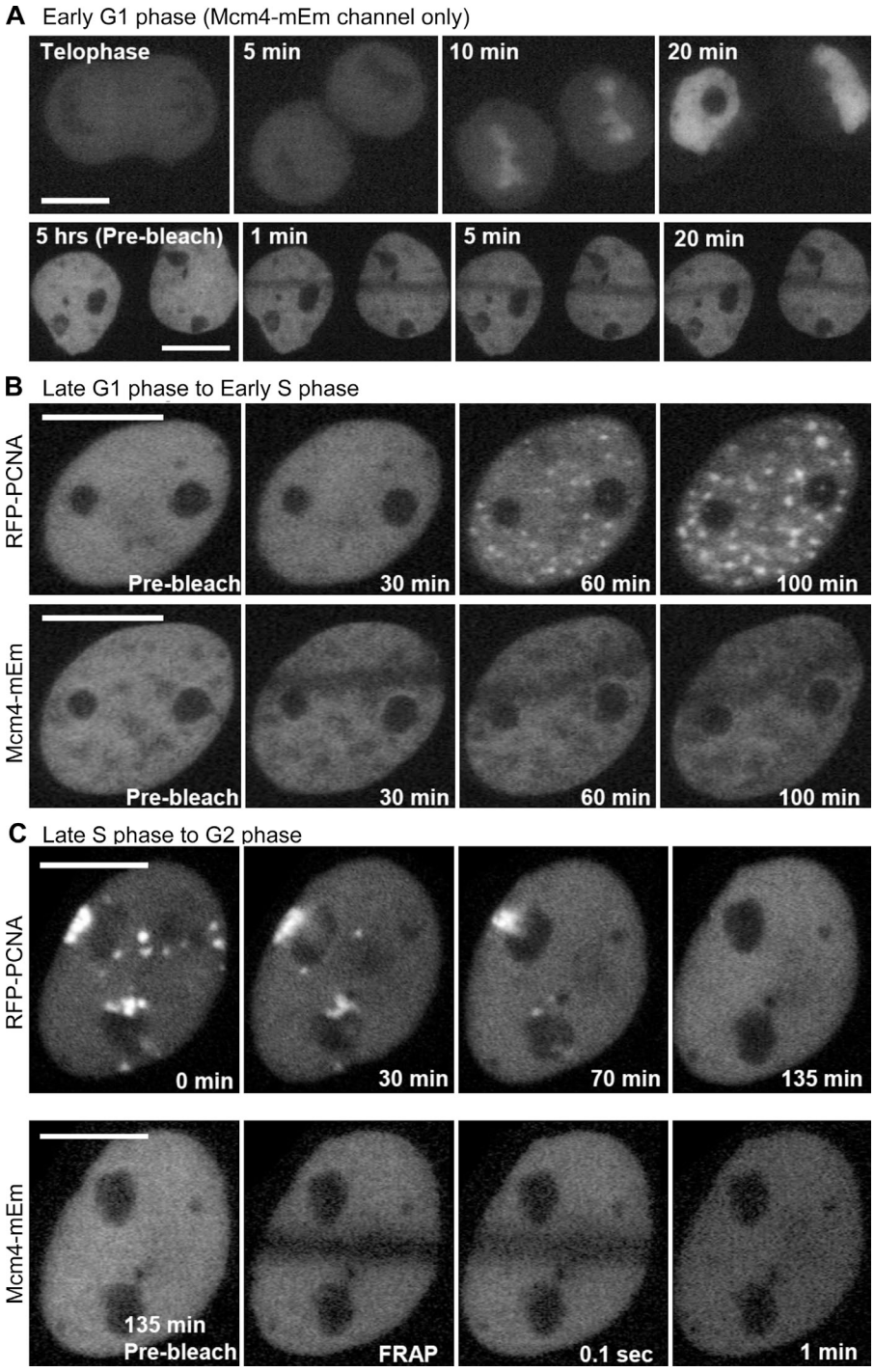

Figure 2. **Protocols for cell cycle–specific FRAP in the absence of drug synchrony.** (A) A cell expressing Mcm4-mEm was imaged emerging from mitosis (top). FRAP experiments were conducted on both sister cells ~5 h later (bottom). (B) A late G1 cell expressing Mcm4-mEm was imaged before a FRAP bleach (Pre-bleach), and at different time points after the bleach to measure recovery. PCNA foci appear between 30 and 60 min, which indicates entry into S phase. (C) A late S phase cell expressing Mcm4-mEm was imaged until all PCNA foci had cleared, followed by a FRAP experiment in the subsequent G2 phase. PCNA foci disappear between 70 and 135 min, which indicated entry into G2 phase. Note that for live cell images, exposure time is minimized to 1/10th of a second, so resolution is compromised. Bars, 10 μm.

be considerably faster than the IF decay time because freely diffusing, unbleached Mcm4 would replace bound, bleached Mcm4 before active unloading. As shown in Fig. 4 B, when the long FRAP experiments in late G1 were averaged together, a clear biphasic recovery was apparent. The fast initial recovery lasted just a few seconds, which is consistent with the diffusion of the mobile, unbleached fraction of Mcm4 into the bleach strip. This fast recovery was then followed by an extended plateau that lasted until the onset of S phase (appearance of PCNA foci; Fig. 4 B, gray bar aligned to time 0), after which a slow, gradual recovery began. This slow, "secondary" recovery was well fit with a line or single weak exponential function that yielded a binding time of ~13.6 h, nearly equivalent to the decay time of the IF. This agreement between the rate of decay of the bound fraction for cells at different times during S phase and the rate of fluorescence recovery for cells monitored during their progression through S phase, both of which match the length of S phase, strongly suggests that Mcm4 FRAP recoveries involve little to no exchange, instead reflecting the unloading of Mcm4 during S phase.

To directly test whether unloading of Mcm4 requires replication, cells were treated with either roscovitine, an inhibitor

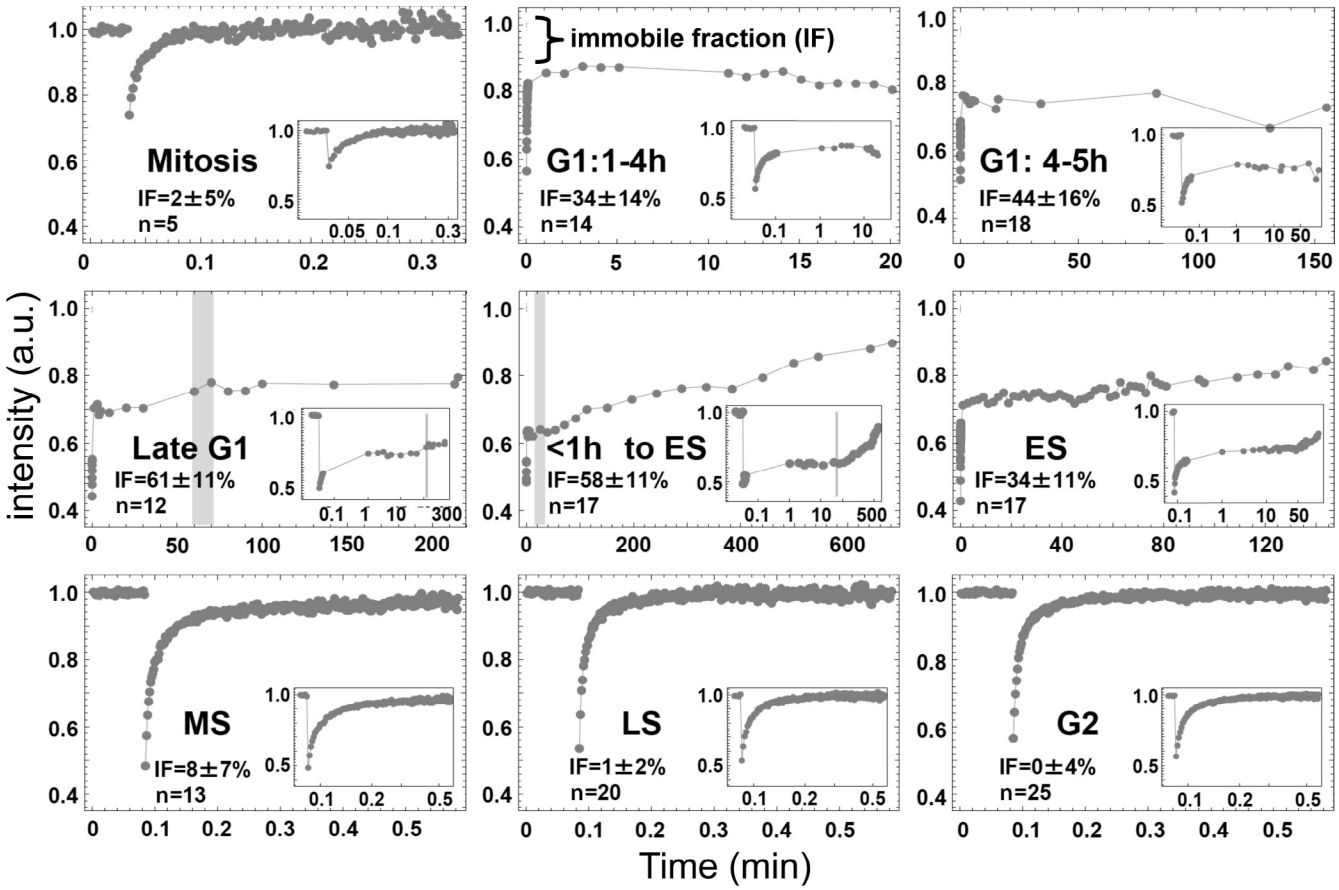

Figure 3. **Cell cycle dependence of Mcm4 recovery.** Mcm4 FRAP recoveries vary significantly throughout the cell cycle. The IF, calculated from the FRAP intensity 30–60 s after bleaching, is minimal after mitosis, but gradually increases to >60% as G1 phase progresses. Once S phase begins, the IF begins to drop, returning to 0% by G2 phase. Inset graphs show the time (x axis) in log scale. *n*, number of cells analyzed to calculate the IF and standard deviation of the mean. The gray bars indicate the initial appearance of PCNA foci.

of Cdk activity necessary for initiation of replication during S phase, or aphidicolin, a direct inhibitor of DNA polymerase. After 24 h of drug treatment, cells in late G1 phase (PCNA foci–negative cells displaying heterogeneous Mcm4-mEm distribution) or very early S (early PCNA foci with heterogeneous Mcm4-mEm distribution), were subjected to FRAP (Fig. 4, C and D). Results revealed undetectable Mcm4-mEm fluorescence recovery of the IF even >3 h after the bleach (Fig. 4 F). Furthermore, FRAP of cells arrested by aphidicolin or roscovitine during S phase indicated an Mcm4-mEm IF consistent with the time at which they were arrested during S phase (as determined by PCNA focal pattern), which is also consistent with Fig. 3 (not depicted).

Finally, we addressed whether the Mcm4-mEm IF within S phase–arrested cells was still irreversibly bound 24 h after cell cycle arrest. Because S phase cells have a large soluble pool of Mcm4-mEm that obscures direct observation of immobilized molecules, we reduced the fluorescence of this soluble pool by subjecting S phase cells to fluorescence loss in photobleaching (FLIP) followed by FRAP (Fig. 4 E). In FLIP, a repeating bleach pulse focused on a small area within the cell nucleus (Fig. 4 E, circles) irreversibly photobleaches most of the mobile Mcm4-mEm (and RFP-PCNA) proteins as they enter the bleaching area, whereas immobilized proteins outside the bleaching area retain their fluorescence. Remarkably, after FLIP erasure of the soluble Mcm4-mEm fluorescence within cells near the middle of S phase, a population of Mcm4-mEm proteins was revealed that was still bound to later replicating chromatin at the nuclear periphery and around the nucleoli. These post-FLIP cells were then subjected to FRAP and the photobleached strip was tracked for >6 h in the continued presence of aphidicolin or roscovitine, revealing no detectable fluorescence recovery of the IF (Fig. 4, E and F). Together, these results demonstrate that Mcm4 remains irreversibly bound to chromatin for >24 h with negligible subunit exchange, and that DNA replication is required to evict fluorescent molecules from unbleached areas of the nucleus into the soluble pool.

Mcm4 is cumulatively loaded onto chromatin during G1 phase

The FRAP experiments in Fig. 3 suggest that Mcm4 loads cumulatively during the course of G1. However, it was also possible that most Mcm4-mEm proteins were tightly bound to chromatin throughout G1 phase, with the increased recovery observed early in G1 phase resulting from chromatin movements (Video 6) that are prevalent during early G1 (Dimitrova and Gilbert, 1999; Chubb and Bickmore, 2003; Cremer and Cremer, 2010). To address this possibility, we established a cell line that stably co-expressed Mcm4-mEm and a histone H2B-mCherry fusion protein, ∼90% of which incorporates stably into chromatin

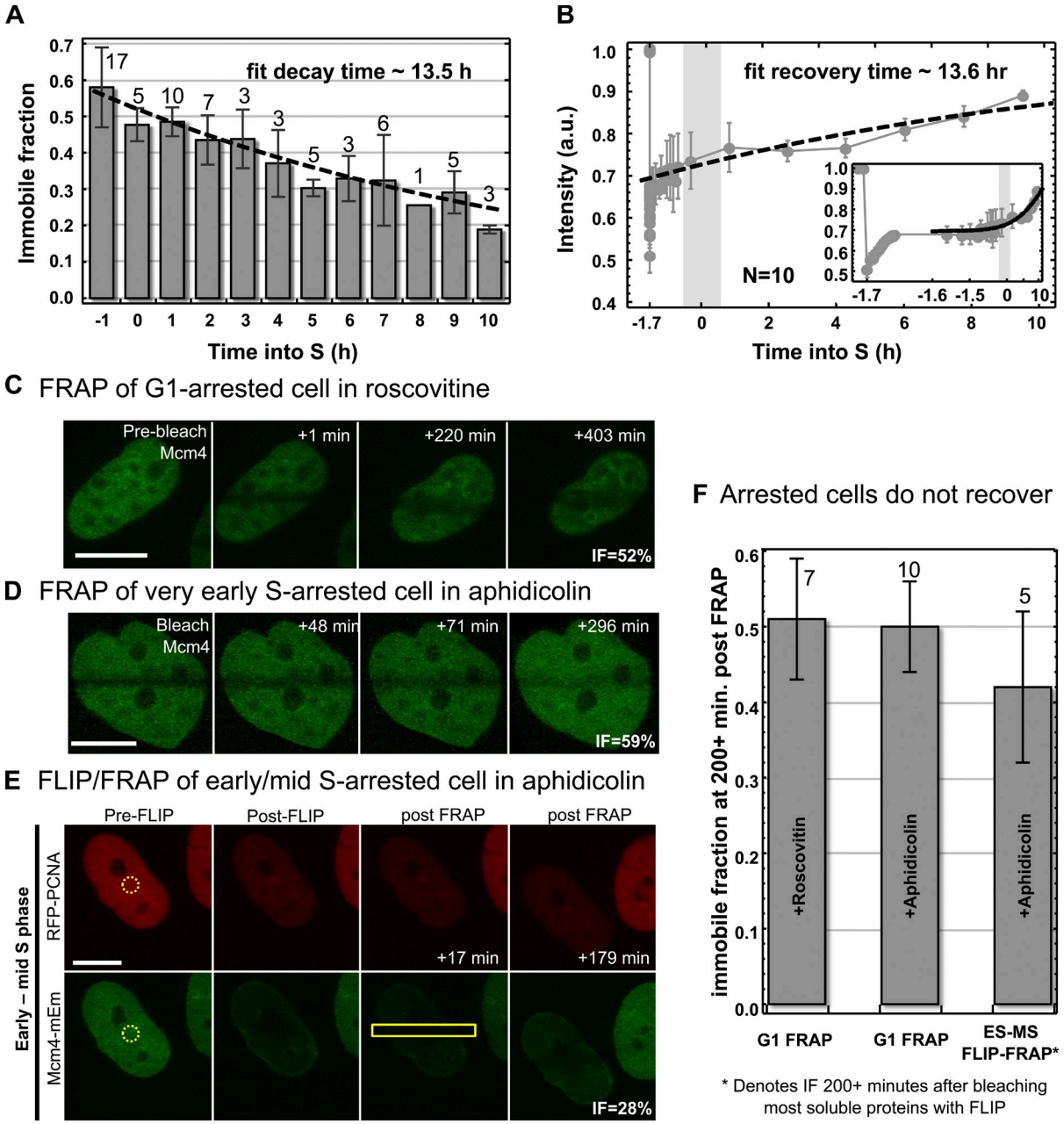

Figure 4. **Mcm4 recovery results from eviction during replication.** (A) The IF was measured from a set of short FRAP experiments (each lasting <1 min) on a pool of cells at various stages of progression through S phase. The mean IF gradually decreased and was well fit by a line or single weak exponential decay (broken line), yielding a decay time of ~13.5 h. The number of cells analyzed for each time interval is shown above the bar. (B) Long FRAP experiments (>150 min each) were performed on 10 cells in G1 phase that were all ~100 min from entering S phase. The mean FRAP recovery after S phase entry was well fit with a line or single weak exponential (broken line), yielding a recovery time of ~13.6 h. The consistency of this recovery time and the IF decay time suggests that Mcm4 undergoes little or no exchange throughout S phase. The gray bar indicates the appearance of PCNA foci. (C–F) Replication arrest prevents Mcm4 unloading. (C) Cells were cultured in roscovitine for 24 h, and a cell lacking PCNA foci but displaying heterogeneous Mcm4-mEm distribution (indicating G1 arrest) was subjected to FRAP and tracked for 403 min with no detectable IF recovery. (D) Cells were cultured in aphidicolin for 24 h, and a cell displaying PCNA foci characteristic of very early S phase as well as heterogeneous Mcm4-mEm distribution (Fig. 1 F) was subjected to FRAP and tracked for 296 min with no detectable IF recovery. (E) A cell cultured in aphidicolin for 24 h and displaying PCNA foci characteristic of early S phase and homogeneous Mcm distribution was subjected to FLIP/FRAP, as described in the text. The FLIP laser was directed in the broken yellow circle, and the FRAP bleach was directed along the solid yellow line. Similar results were obtained with roscovitine-arrested cells. Note that, although we observed a substantial reduction in the intensity of PCNA foci during aphidicolin arrest, as described previously (Görisch et al., 2008), characteristic focal patterns of PCNA were still discernable. Bars, 10 µm. (F) Quantification of the average bound fractions for groups of cells treated and analyzed as illustrated in C–E, and imaged for a minimum of 200 min. The number of cells analyzed and the standard deviation of the mean are shown above each bar (error bars). FRAP curves similar to those shown in Fig. 3 showed no recovery of the IF throughout the imaging period, so the bound fraction at the end of the entire imaging period is shown for simplicity. Note that for FLIP/FRAP of cells in early to mid S phase (ES/MS), the IF is actually considerably lower, but is measured after a significant fraction of the soluble molecules have been bleached.

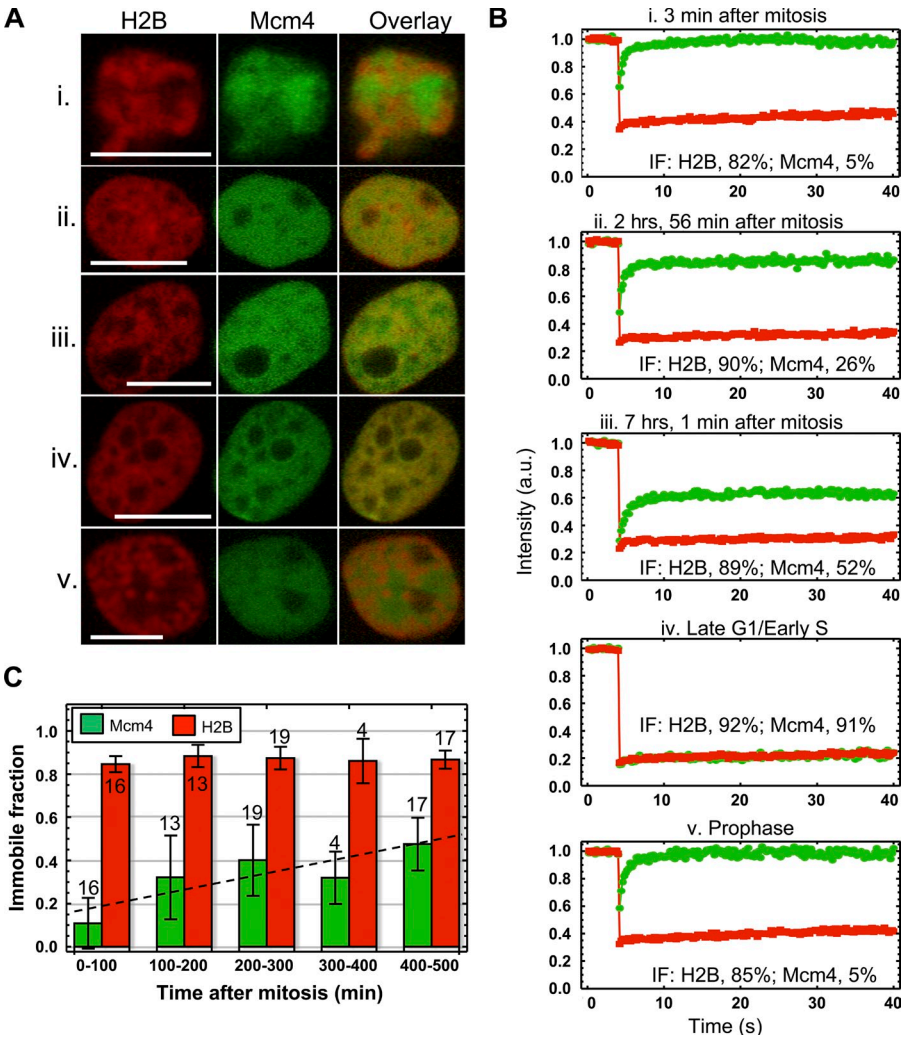

Figure 5. **Mcm4 is cumulatively loaded onto chromatin throughout G1 phase.** (A) A cell line stably expressing Mcm4-mEm and H2B-mCherry fusion proteins was established, and FRAP experiments were conducted at various times after mitosis (operationally defined here as the time at which Mcm4 was observed to reenter the cell nucleus after nuclear membrane reformation). H2B, Mcm4, and overlay images are shown for five representative cells (i–v) at different time points after mitosis. Bars, 10 µm. (B) FRAP curves and IFs for H2B-mCherry and Mcm4-mEm are shown for the five representative cells in A. (C) Using the Mcm4-mEm/H2B-mCherry cell line, 71 cells underwent FRAP experiments between 0 and ~500 min after mitosis, and the IF was calculated for both Mcm4 and H2B. Although it is difficult to track the entire length of G1 phase by this method, a linear slope fit (broken line) to all 71 data points would extrapolate to ~70% Mcm4 loaded by 700 min, which is close to the length of G1 phase and is consistent with cells deemed to be in very late G1 phase by H2B colocalization (Fig. S5 B).

throughout the cell cycle (Kimura and Cook, 2001). FRAP experiments were performed on cells at different times during G1 (Video 7), and the recovery of Mcm4-mEm versus H2B fluorescence was compared (Fig. 5). When Mcm first entered the nucleus (Fig. 5 A, i), it did not immediately colocalize with H2B but was excluded from chromatin and exhibited little or no IF (Fig. 5 B, i), whereas 80% of H2B remained immobile. Hence, the degree of chromatin mobility during the very early G1 phase period is not sufficient to explain the rapid and nearly complete Mcm4 FRAP recovery at this time. During the course of G1 phase, however, there was a gradual and cumulative increase in the Mcm4-mEm IF (Fig. 5, B and C), accompanied by an increased colocalization of Mcm4 with H2B (Fig. 5 A, i–iii). In fact, some cells could be identified that showed a high degree of colocalization between Mcm4 and H2B, and within these cells, the Mcm4 IF was nearly as high as H2B (Fig. 5 A, iv; Fig. 5 B, iv; Fig. S5; and Video 7). We did not have PCNA to track cells through S phase and into G2 phase, but we could identify cells in early mitosis (prophase) based on the condensation of chromatin (which was confirmed by entry into mitosis after FRAP; Fig. S4). In prophase cells, Mcm4-mEm did not colocalize with H2B but was excluded from chromatin and exhibited little or no IF, whereas H2B remained tightly bound (Fig. 5 A, v; Fig. 5 B, v; Fig. S5; and Video 8). Together, these results indicate that Mcm4 is loaded onto chromatin gradually and cumulatively throughout G1 phase and reaches a maximum of >70% (Fig. S5) bound just before the entry into S phase.

We next asked whether the continuous loading of Mcm proteins during G1 phase required progression through defined G1 phase hallmarks. For example, the origin decision point (ODP) is a time when specific sites are selected for initiation of replication (Wu and Gilbert, 1996; Sasaki et al., 2006) and the restriction point (R point) marks the commitment to initiate replication independent of mitogenic stimuli (Wu and Gilbert, 1997). Cells treated with roscovitine or the protein synthesis inhibitor cycloheximide as they exit from mitosis will arrest either before the ODP or between the ODP and the R point, respectively (Keezer and Gilbert, 2002). Neither treatment had any effect on FRAP recovery of Mcm4-mEm or the cumulative loading of Mcm4-mEm throughout G1 phase (Fig. S5, C and D).

Lack of colocalization of Mcm4 with PCNA coincides with chromatin decondensation

As mentioned in the Introduction, a longstanding paradox has been why Mcm helicase subunits do not colocalize with other replication fork proteins (Todorov et al., 1995; Krude et al., 1996; Romanowski et al., 1996; Dimitrova et al., 1999). These results were obtained with cells that were first detergent-extracted,

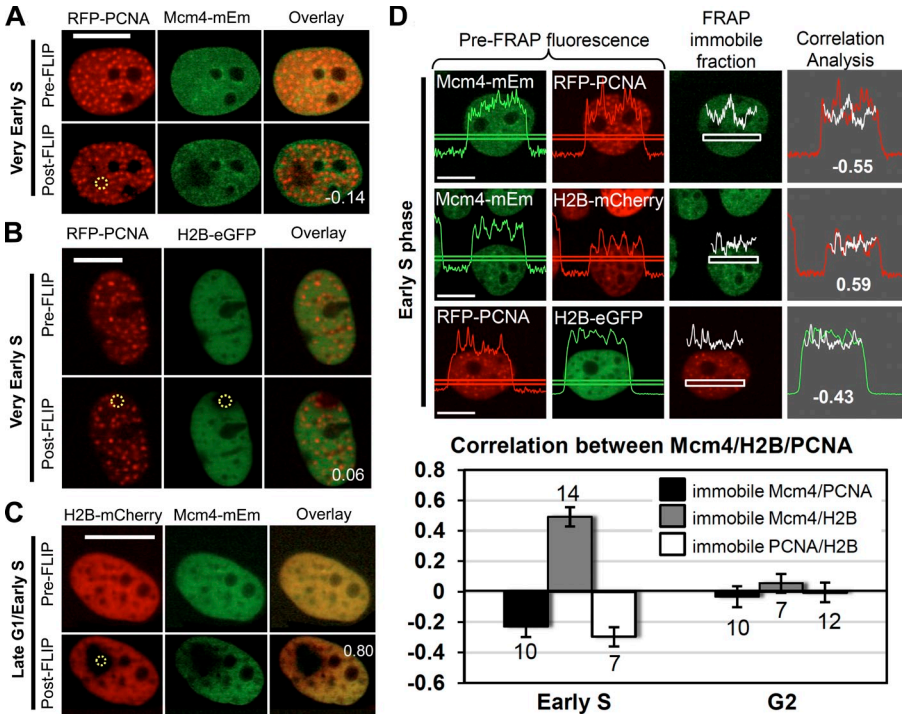

Figure 6. **Sites of DNA synthesis are sites of low chromatin and Mcm4 density.** (A) Lack of colocalization of PCNA and Mcm proteins in living cells. Mcm4-mEm/RFP-PCNA–expressing cells in very early S phase were subjected to FLIP to reduce the fluorescence of the soluble pool of molecules as in Fig. 4. After FLIP, colocalization analysis of the immobile Mcm4-mEm and RFP-PCNA fractions was performed, and the correlation coefficient is indicated in the Post-FLIP overlay. (B and C) Similar FLIP colocalization analysis for RFP-PCNA/H2B-mCherry (B)- and Mcm4-mEm/H2B-mCherry (C)-expressing cells. The yellow circles represent where the FLIP laser (488 nm) was directed. (D) Strip FRAP was performed in cells stably expressing Mcm4-mEm/RFP-PCNA (top), Mcm4-mEm/H2B-mCherry (middle), and H2B-eGFP/RFP-PCNA (bottom) in early S and G2 phase. In each experiment, the IF was measured along the length of the bleach strip (third column), and this was correlated (via Pearson's correlation coefficient, fourth column) with the prebleach fluorescence along the bleach strip (first two columns). Mean results are shown together with the standard error of the mean (error bars with number of cells for each displayed) in the bar plot below. Bars, 10 µm.

which is necessary to remove soluble Mcm and PCNA proteins that obscure efforts to localize these proteins (Dimitrova et al., 1999; Dimitrova and Gilbert, 2000) before fixation and immunohistochemistry. We wished to confirm whether a lack of colocalization could also be observed in living cells without detergent extraction and fixation. As expected, the soluble Mcm and PCNA proteins obscured our ability to evaluate colocalization, but the fluorescence of the soluble pool could be reduced by FLIP (as in Fig. 4), which showed that Mcm4-mEm and RFP-PCNA proteins do not colocalize even in living cells (Fig. 6 A).

A hypothesis to explain this paradox is that a large amount of excess "loosely bound" Mcm complexes might be cleared from chromatin upon the assembly of replication forks, leaving behind only a few active Mcm helicases at the replication fork and giving the appearance of a lack of colocalization (Dimitrova et al., 1999). However, this hypothesis is inconsistent with the need to retain those excess Mcm complexes to function as dormant origins under conditions of replicational stress (Ge et al., 2007; Gilbert, 2007; Ibarra et al., 2008). Our results demonstrating a tight linkage between Mcm4-mEm and chromatin suggest an alternative hypothesis. Sites of active replication visualized by electron microscopy have been observed to contain a very low density of DNA (Philimonenko et al., 2004). We reasoned that if the assembly of replication forks, visualized by the appearance of PCNA foci, were to result in a local but extensive decondensation of chromatin, then the tightly bound Mcm proteins would also decondense and be considerably reduced in concentration. To test this hypothesis, we constructed a cell line coexpressing RFP-PCNA and H2B-EGFP and performed FLIP/colocalization experiments in both this cell line and our Mcm4-mEm/H2B-mCherry cell line described in Fig. 5. Results revealed that PCNA foci did not correlate with the density of chromatin (Fig. 6 B), whereas a close colocalization between Mcm4 and H2B was observed during late G1/early S phase (Fig. 6 C).

To confirm this result using a method that did not require bleaching out the soluble pool of molecules, we performed FRAP experiments in cell lines containing each of the pairwise combinations of these three proteins and correlated the locations of the immobilized fractions of these proteins across the bleached area (Fig. 6 D). We found that although the IFs of Mcm4 and H2B were strongly correlated, the immobilized fraction of PCNA negatively correlated with either Mcm4 or H2B (Fig. 6 D), which indicates that immobile Mcm4-mEm is depleted in areas of PCNA that are also depleted of chromatin. Altogether, our results suggest that replication foci are regions of decondensed chromatin that consequently reduce the density of chromatin-bound Mcm relative to the remaining unreplicated chromatin throughout the nucleus. PCNA (and other replication proteins), in contrast, is bound exclusively at the sites of DNA synthesis and shows strong enrichment at those sites.

Behavior of the other Mcm subunits

Similar FRAP experiments were performed with Mcm-mEm/RFP-PCNA cell lines expressing tagged Mcm2, -3, -6, and -7. As summarized in Fig. 7, Mcm2 and -6 behaved qualitatively and quantitatively similar to Mcm4, whereas Mcm3 and -7 were qualitatively similar but had a lower IF compared with Mcm 2, -4, and -6. This quantitative difference for Mcm3 and -7 may be caused by an impaired ability of the tagged Mcm3 and -7 proteins to incorporate into chromatin-bound Mcm complexes. In fact, tagged Mcm3 and -7 were more detergent-extractable than endogenous Mcms (Fig. S4 E), unlike tagged Mcm4 (Fig. 1 C). Nonetheless, all five subunits show similar cell cycle regulation of a tight chromatin binding fraction, which strongly suggests that our detailed analysis of Mcm4-mEm is representative of the hetero-hexameric Mcm complex.

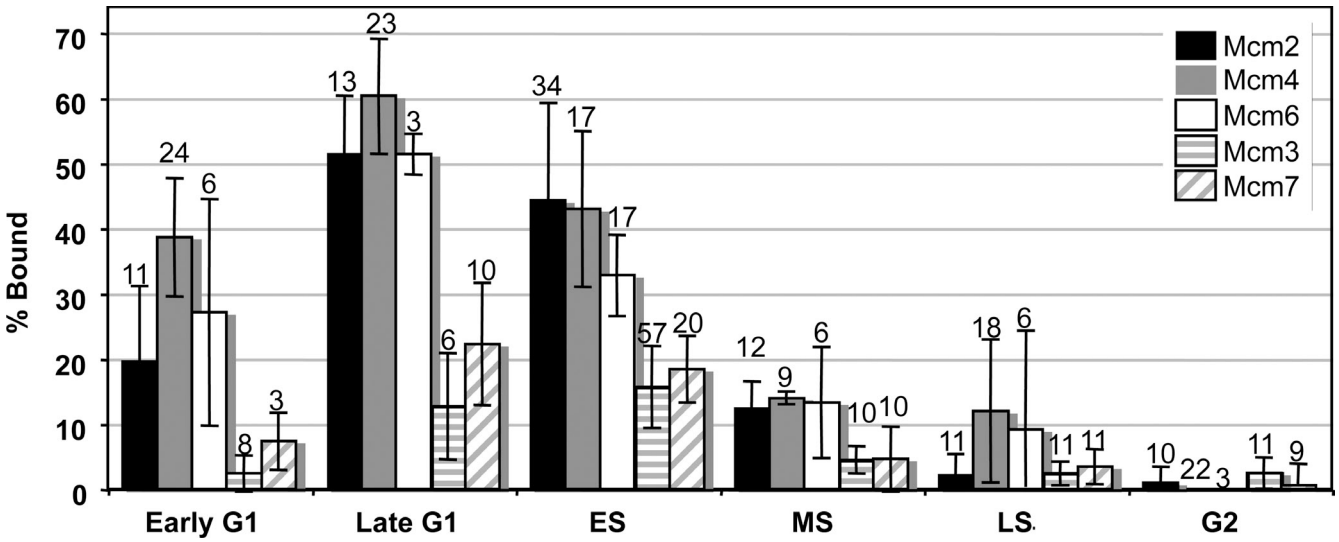

Figure 7. **Other Mcm subunits also display a cell cycle dependence of the IF.** Mcm2-, Mcm3-, Mcm4-, Mcm6-, or Mcm7-mEm cells were tracked out of mitosis, and FRAP experiments were conducted at various times in the cell cycle. The immobile Mcm fraction was calculated from each FRAP curve, and the data were binned according to the subunit and the number of minutes after mitosis. The number of cells analyzed for each cell cycle stage and the standard deviation of the mean are shown at the top of each bar (error bars).

Discussion

Here we have studied, in vivo, the interactions of the Mcm2, -3, -4, -6, and -7 proteins with chromatin. We show that these five subunits exhibit static interactions with chromatin, in contrast to the dynamic interactions seen with other replication proteins (McNairn et al., 2005; Xouri et al., 2007) and almost all nonhistone proteins (Phair and Misteli, 2000; Misteli, 2001; Hager et al., 2009). This is consistent with the in vivo existence of an Mcm complex topologically linked to DNA as previously demonstrated in vitro (Evrin et al., 2009; Remus et al., 2009). Our data also suggest that the lack of colocalization of Mcm proteins with other replication fork proteins results from a decondensation of chromatin and a relative dilution of immobilized Mcm proteins at sites of DNA synthesis. We propose that the nondynamic state of Mcm2-7 interaction on chromatin from G1 phase through initiation during S phase permits the retention of Mcm complexes during the long temporal separation between replication licensing and initiation, and is necessary to ensure complete and timely duplication of the genome while preventing any possibility of rereplication.

Lockdown/kickoff: a topologically linked liaison that is unlinked by replication?

We previously demonstrated that the physical association of Mcm with chromatin during telophase is sufficient to license chromatin for a round of replication in *Xenopus laevis* egg extracts that lack either Mcm proteins or are inhibited for the assembly of preRCs (Okuno et al., 2001; Dimitrova et al., 2002), which provided direct evidence that this in vivo association is functional. Here, we present evidence that the association of Mcms during early G1 phase represents an irreversible link. This result alone is significant, as virtually all previously studied chromatin-binding proteins exchange on and off chromatin in seconds or minutes (Phair and Misteli, 2000), including the preRC components ORC (McNairn et al., 2005) and Cdt1 (Xouri et al., 2007) and replication fork proteins PCNA and RPA (Fig. S2 E; Görisch et al., 2008). Only histones (Kimura and Cook, 2001) and cohesins (Gerlich et al., 2006) have residence times approaching what we find for Mcms. Once replication begins, the Mcm complexes are unloaded into a soluble form, and our results suggest that the passage of replication forks is necessary to actively remove bound Mcm proteins from chromatin. During S phase, the decrease in bound Mcm fit to a linear or weak single exponential decay, yielding a decay time and recovery time of roughly the same value, which was equivalent to the mean length of S phase. The consistency of the IF decay time and recovery time suggests that Mcm4 undergoes little or no exchange throughout S phase, and that Mcm clearing requires replication. In fact, when DNA synthesis was inhibited, loaded Mcm complexes remained bound indefinitely. This indicates that the myriad chromatin activities that continue during normal G1 phase or during a replication arrest, such as chromatin remodeling and transcription, do not displace the Mcm complexes to any significant extent.

We did not detect any transiently immobilized fraction of Mcm4-mEm in our analyses despite a rigorous search for exchange. This indicates that if Mcm2-7 complexes are loaded via a "docked" or "associated" intermediate, as suggested from in vitro studies (Evrin et al., 2009; Francis et al., 2009; Remus et al., 2009; Tsakraklides and Bell, 2010), then the fraction of such complexes in this intermediate state is too small (<5%) to be detected in our experiments. This suggests that this intermediate is short-lived in the living cell environment. Further investigation will be needed to determine whether culture conditions or mutations in fluorescent Mcm proteins can be identified that are capable of trapping this intermediate. In addition, we found that Mcm proteins load continuously during G1 phase, and we did not find any evidence of a change in the stability of the Mcm–chromatin interaction during origin choice at the ODP or

during commitment to S phase at the R point. This favors models in which the ODP selects a subset of loaded Mcms for initiation (Sasaki et al., 2006). It also implies that Mcms are in the loaded form before the decision to enter S phase or exit the cell cycle. Hence, it will be interesting to determine how Mcm complex disassembly occurs during exit from the cell cycle into quiescence and senescence (Stoeber et al., 2001; Harada et al., 2008).

A resolution to the paradox of Mcm absence at replication foci

We have confirmed in living cells the lack of colocalization of Mcm with replication fork proteins previously observed by immunohistochemistry (Todorov et al., 1995; Krude et al., 1996; Romanowski et al., 1996; Dimitrova et al., 1999), and our results suggest a novel hypothesis to explain this paradox. We find that sites of DNA synthesis, typified by the formation of punctate foci of transiently immobilized PCNA, colocalize with sites of decondensed or low-density chromatin, whereas the density of immobilized Mcm proteins tracks closely with chromatin. Moreover, Mcm FRAP recovery is most rapid in the regions of PCNA foci and decondensed where the Mcm IF is relatively low in Fig. 6 D, which suggests that decondensed chromatin at sites of ongoing replication provides space for unbleached, soluble Mcm proteins to enter by diffusion. Our results demonstrate that decondensation of chromatin reduces the local concentration of loaded Mcm complexes, whereas other replication proteins are enriched exclusively at these sites, providing a satisfying explanation for the long-observed lack of colocalization of Mcms with proteins recruited to the replication fork during ongoing DNA synthesis.

Materials and methods

Construction of expression plasmids

An in-frame fusion to the C terminus of mEm was generated as follows: *Mus musculus* Mcm2-7 sequences (provided by H. Kimura, Graduate School of Frontier Biosciences, Osaka University, Osaka, Japan) were amplified by PCR, and the resulting PCR product was ligated into a vector backbone containing the mEmerald (Shaner et al., 2007) sequence, followed by the biotin ligase tag (BLT; Beckett et al., 1999). A flexible linker (Leonhardt et al., 2000) was inserted between the Mcm DNA and the fluorescent tag, and between the fluorescent tag and the BLT, to aid in fusion folding and functionality. Each fusion was under the control of a tet promoter (Izumi and Gilbert, 1999). Each fusion was verified by sequencing. See Fig. S1 (A and B) for a listing of plasmid constructs.

Cell line construction and synchrony

CHO cells stably expressing tTA (Izumi and Gilbert, 1999) were grown in DME (catalog No. 12100–061; Invitrogen) supplemented with 10% FBS (Invitrogen), penicillin/streptomycin (catalog No. 30-002-CI; Cellgro), and MEM Nonessential Amino Acids (catalog No. 25-025-CI; Cellgro). BirA was transfected into the tTA-expressing cell line using Effectene (catalog No. 301427; QIAGEN). A stable BirA-expressing cell line was selected with 2.5 µg/ml blasticidin (Invitrogen). pRMCE_Mcm-mEmerald-BLT vectors were transfected into the tTA/BirA-expressing cell line using Effectene. Stable Mcm cell lines were selected with 400 µg/ml Zeocin (Invitrogen) and screened for fluorescence using an inverted fluorescence microscope. Mcm-mEmerald–expressing cell lines were transfected with RFP-PCNA (provided by C. Cardoso, Technische Universität Darmstadt, Darmstadt, Germany; Leonhardt et al., 2000) or H2B-mCherry (Kimura and Cook, 2001), and stable cell lines were selected with 400 µg/ml G418 (EMD) and screened for fluorescence using an inverted fluorescence microscope. See Fig. S1C for a listing of all constructed mEmerald cell lines.

Tet-regulatable fusion protein cell lines were maintained in DME supplemented with 10% FBS, penicillin/streptomycin, MEM nonessential amino acids, 400 µg/ml Zeocin (for Mcm selection), 400 µg/ml G418 (for PCNA or H2B selection), 500 µg/ml Hygromycin B (for tTA selection; Invitrogen), and 2.5 µg/ml Blasticidin (for BirA selection).

To synchronize cells in mitosis for biochemical studies, 0.05 µg/ml nocodazole was added to the media for 4 h followed by mechanical shake-off. Metaphase spread analysis indicated that >95% mitotic cells were routinely obtained. 40 µM roscovitine (EMD) and 10 µg/ml aphidicolin (EMD) were used, where indicated.

Indirect immunofluorescence microscopy

Cells of each of the Mcm/PCNA-expressing stable cell lines were grown on coverslips, washed with cold 1× PBS (10× PBS: 137 mM NaCl, 2.7 mM KCl, 10 mM Na_2HPO_4, and 2 mM KH_2PO_4) followed by ice-cold CSK buffer (10 mM Hepes-KOH, pH 7.4, 300 mM sucrose, 100 mM NaCl, and 3 mM $MgCl_2$), and extracted with 0.5% Triton X-100 in CSK supplemented with protease inhibitors (1:50, Cocktail III, No. 539134; VWR) for 2 min on ice. Coverslips were washed with PBS three times and fixed for 20 min at room temperature with 2% paraformaldehyde in PBS. After fixation, coverslips underwent the following ordered washes: PBS, 0.5% NP-40 in PBS, 0.5% Tween-20 in PBS, and 0.5% Tween-20 in PBS with 3% BSA. Coverslips were then incubated with BM28 (Mcm2) primary antibody at a 1:50 dilution for 1 h at room temperature. Coverslips were next washed three times with 0.5% Tween-20 in PBS, and incubated in secondary antibody in PBS, 0.5% Tween-20, and 3% BSA for 1 h at room temperature. Coverslips then underwent the following ordered washes: 0.5% Tween-20 in PBS, PBS and DAPI, and distilled water. Coverslips were then mounted on slides with Celvatol for viewing with the microscope (Ti-U Eclipse; Nikon). Images (Figs. 2 B and S2 A) were viewed using a 60×, 1.4 NA oil immersion lens, and captured with NIS Elements using a digital camera (model No. C4742-95; Hamamatsu Photonics), and adjusted with only contrast and brightness adjustments. For Mcm/RFP-PCNA extraction photos, BM28 antibody staining was omitted. CoLocalizer Express (CoLocalization Research Software) was used for all quantitative colocalization analysis.

Western blotting and coimmunoprecipitation

Streptavidin–Sepharose 4B beads (Invitrogen) and/or the GFP-Trap (Rothbauer et al., 2008) from ChromoTek were used to show coimmunoprecipitation of the fluorescently tagged Mcm proteins with endogenous Mcm subunits. For soluble coimmunoprecipitation, 10^7 cells were resuspended in 200 µl of lysis buffer (10 mM Tris/Cl, pH 7.5, 150 mM NaCl, 0.5 mM EDTA, 0.5% NP-40, 1 mM PMSF added freshly, and 1× protease inhibitors Cocktail III) and placed on ice for 30 min with extensive pipetting every 10 min. The cell lysates were spun for 10 min at 13,000 *g* at 4°C. The supernatant was transferred to a precooled tube, and the volume was adjusted to 500 µl with dilution buffer (10 mM Tris/Cl, pH 7.5, 150 mM NaCl, 0.5 mM EDTA, 1 mM PMSF freshly added, and 1× protease inhibitor Cocktail III). 20 µl of equilibrated beads (which had been blocked overnight at 4°C with rotation in 0.1 mg/ml BSA) were added to the cell lysate and incubated with gentle end-over-end mixing for 1 h at 4°C. Beads were washed with 250 µl of cold dilution buffer three times, and the beads were resuspended in 100 µl of hot 2× SDS sample buffer (125 mM Tris, pH 6.8, 4% SDS, 10% glycerol, 0.006% bromophenol blue, and 1.8% β-mercaptoethanol) and boiled. Sample input, supernatant (unbound), and final sample (bound) were analyzed by Western blotting (Rothbauer et al., 2008). For chromatin pull-down, the Nuclear Complex Co-IP kit (catalog No. 54001; Active Motif) was used with the accompanying protocol. Antibodies used were as follows: BM28 (material No. 610700; BD) at 1:10,000 in 1% BSA/0.3% nonfat dry milk (NFDM); Mcm3 (catalog No. 4012; Cell Signaling Technology) at 1:10,000 in 5% BSA; Mcm4 (sc-48407; Santa Cruz Biotechnology, Inc.) at 1:200 in 1% NFDM; Mcm5 (sc-22780; Santa Cruz Biotechnology, Inc.) at 1:20,000 in 5% NFDM; Mcm6 (sc-55577; Santa Cruz Biotechnology, Inc.) at 1:200 in 5% NFDM; Mcm7 (sc-9966; Santa Cruz Biotechnology, Inc.) at 1:15,000 in 1% NFDM; β-tubulin (Sigma-Aldrich) at 1:10,000 in 5% NFDM; LaminB (sc-6216; Santa Cruz Biotechnology, Inc.) at 1:1,000 in 5% NFM; and anti-PCNA (Oncogene) at 1:3,000 in 1% BSA/0.3% NFDM.

Live cell imaging

Low-power imaging of cells to identify colonies (Fig. 1 B) was done directly on the cell culture dish with a microscope (Ti-U Eclipse) using a 20×, 0.4 NA lens in fluorescence and phase-contrast channels. Images were captured with NIS Elements using a digital camera (model No. C4742-95; Hamamatsu Photonics) and adjusted with only contrast and brightness adjustments. Long-term imaging Videos 1 and 2 were performed with an incubator fluorescence microscope (VivaView; Olympus), with cells growing

on MatTek dishes at 37°C, using a 40×, NA 0.95 lens. Images were captured with a charge-coupled device camera using MetaMorph software (MDS Analytical Technologies), and cropping was performed using ImageJ (National Institutes of Health, http://rsb.info.nih.gov/ij/). All other live imaging, including all photobleaching experiments, were performed on a laser scanning microscope (LSM 5 Live DuoScan; Carl Zeiss, Inc.) equipped with a 63×/1.4 NA oil immersion lens and a line CCD, and images were captured with the ZEN software package (Carl Zeiss, Inc.). The temperature during experiments was maintained at 37°C using the Delta-T live cell imaging system from Bioptechs. mEmerald, RFP, and mCherry fluorescent proteins were excited using the 489- and 594-nm laser lines, respectively. Either 20 or 50 prebleach images were recorded with 8% laser power of the 489-nm line followed by a bleach pulse of one iteration, scan speed 3, for a pixel dwell time of 51.2 µs of the 489-nm laser line set at 100%. After bleaching, either 300 postbleach images were collected at 10 frames per second, or imaging was reduced to upwards of 1 min between frames to minimize photobleaching and to enable the imaging of longer FRAPs. Background intensities were subtracted from each image before analysis using ImageJ. To allow the direct comparison between FRAP curves, raw data were normalized as follows: the average fluorescent intensity of each cell nucleus and each strip-FRAP area was calculated using ImageJ's polygon selection and measuring tool, and the strip-FRAP average intensity was divided by the cell nucleus average intensity to give a normalized value (FRAP/cell); each normalized value was then divided by the preintensity average (calculated as the mean of the prebleach normalized values), and these values were plotted (y axis) against time (x axis). The FRAP IF was calculated as the percentage of nonrecovered fluorescence 30 s to ∼1 min after bleaching (by 30 s, the fast, diffusive part of recoveries was complete and the recovery curves were nearly flat on the time scale of seconds). CoLocalizer Express was used for all quantitative colocalization analysis.

Online supplemental material

Fig. S1 shows the plasmids and cell lines constructed. Fig. S2 shows an additional characterization of the Mcm4-mEm/RFP-PCNA cell line. Fig. S3 shows a characterization of total Mcm-mEm. Fig. S4 shows a characterization of chromatin-bound Mcm-mEm. Fig. S5 shows additional analyses of Mcm4-mEm/H2B-Cherry cell line. Video 1 shows long-term imaging of a cell going from mitosis to S phase in ∼10 h. Video 2 shows long-term imaging of a cell going through an entire S phase in ∼13.5 h. Video 3 shows that Mcm4-mEm localizes to the nucleus upon exit from mitosis. Video 4 shows that Mcm4-mEm displays "chromatin-like" look in late G1, before PCNA foci formation. Video 5 shows that the IF of Mcm4 decreases as S phase progresses. Video 6 shows that chromatin undergoes many movements in mitosis and early G1, as visualized by H2B-mCherry. Video 7 show that IFs of Mcm4-mEm and H2B-mCherry mirror each other in late G1 and early S phase. Video 8 shows that H2B has a high IF in G2/prometaphase, but not Mcm4. Video 9 show that RFP-PCNA foci recover in ∼15 min, whereas the soluble portion of RFP-PCNA recovers quickly. Online supplemental material is available at http://www.jcb.org/cgi/content/full/jcb.201007111/DC1.

We thank R. Didier for assistance with flow cytometry, H. Kimura for helpful comments on the manuscript and for mouse cDNA plasmids for Mcm2-7, C. Cardoso for GFP and RFP human PCNA plasmids, H. Masai for mouse Mcm4 mutant 6AA plasmid, J. Schimenti for Mcm4 mutant Chaos3 plasmid, and A. Schwacha and T. Misteli for helpful discussions. This work was supported by National Institute for General Medical Sciences grant RO1GM083337 to D.M. Gilbert.

Submitted: 20 July 2010
Accepted: 19 November 2010

References

Beckett, D., E. Kovaleva, and P.J. Schatz. 1999. A minimal peptide substrate in biotin holoenzyme synthetase-catalyzed biotinylation. *Protein Sci.* 8:921–929. doi:10.1110/ps.8.4.921

Bousset, K., and J.F. Diffley. 1998. The Cdc7 protein kinase is required for origin firing during S phase. *Genes Dev.* 12:480–490. doi:10.1101/gad.12.4.480

Chubb, J.R., and W.A. Bickmore. 2003. Considering nuclear compartmentalization in the light of nuclear dynamics. *Cell.* 112:403–406. doi:10.1016/S0092-8674(03)00078-3

Cremer, T., and M. Cremer. 2010. Chromosome territories. *Cold Spring Harb Perspect Biol.* 2:a003889. doi:10.1101/cshperspect.a003889

DaFonseca, C.J., F. Shu, and J.J. Zhang. 2001. Identification of two residues in MCM5 critical for the assembly of MCM complexes and Stat1-mediated transcription activation in response to IFN-gamma. *Proc. Natl. Acad. Sci. USA.* 98:3034–3039. doi:10.1073/pnas.061487598

de Boer, E., P. Rodriguez, E. Bonte, J. Krijgsveld, E. Katsantoni, A. Heck, F. Grosveld, and J. Strouboulis. 2003. Efficient biotinylation and single-step purification of tagged transcription factors in mammalian cells and transgenic mice. *Proc. Natl. Acad. Sci. USA.* 100:7480–7485. doi:10.1073/pnas.1332608100

Deal, R.B., J.G. Henikoff, and S. Henikoff. 2010. Genome-wide kinetics of nucleosome turnover determined by metabolic labeling of histones. *Science.* 328:1161–1164. doi:10.1126/science.1186777

Dimitrova, D.S., and D.M. Gilbert. 1999. The spatial position and replication timing of chromosomal domains are both established in early G1 phase. *Mol. Cell.* 4:983–993. doi:10.1016/S1097-2765(00)80227-0

Dimitrova, D.S., and D.M. Gilbert. 2000. Stability and nuclear distribution of mammalian replication protein A heterotrimeric complex. *Exp. Cell Res.* 254:321–327. doi:10.1006/excr.1999.4770

Dimitrova, D.S., I.T. Todorov, T. Melendy, and D.M. Gilbert. 1999. Mcm2, but not RPA, is a component of the mammalian early G1-phase prereplication complex. *J. Cell Biol.* 146:709–722. doi:10.1083/jcb.146.4.709

Dimitrova, D.S., T.A. Prokhorova, J.J. Blow, I.T. Todorov, and D.M. Gilbert. 2002. Mammalian nuclei become licensed for DNA replication during late telophase. *J. Cell Sci.* 115:51–59. doi:10.1242/jcs.00087

Donaldson, A.D., W.L. Fangman, and B.J. Brewer. 1998. Cdc7 is required throughout the yeast S phase to activate replication origins. *Genes Dev.* 12:491–501. doi:10.1101/gad.12.4.491

Edwards, M.C., A.V. Tutter, C. Cvetic, C.H. Gilbert, T.A. Prokhorova, and J.C. Walter. 2002. MCM2-7 complexes bind chromatin in a distributed pattern surrounding the origin recognition complex in *Xenopus* egg extracts. *J. Biol. Chem.* 277:33049–33057. doi:10.1074/jbc.M204438200

Essers, J., A.F. Theil, C. Baldeyron, W.A. van Cappellen, A.B. Houtsmuller, R. Kanaar, and W. Vermeulen. 2005. Nuclear dynamics of PCNA in DNA replication and repair. *Mol. Cell. Biol.* 25:9350–9359. doi:10.1128/MCB.25.21.9350-9359.2005

Evrin, C., P. Clarke, J. Zech, R. Lurz, J. Sun, S. Uhle, H. Li, B. Stillman, and C. Speck. 2009. A double-hexameric MCM2-7 complex is loaded onto origin DNA during licensing of eukaryotic DNA replication. *Proc. Natl. Acad. Sci. USA.* 106:20240–20245. doi:10.1073/pnas.0911500106

Ferguson, R.L., and J.L. Maller. 2008. Cyclin E-dependent localization of MCM5 regulates centrosome duplication. *J. Cell Sci.* 121:3224–3232. doi:10.1242/jcs.034702

Francis, L.I., J.C. Randell, T.J. Takara, L. Uchima, and S.P. Bell. 2009. Incorporation into the prereplicative complex activates the Mcm2-7 helicase for Cdc7-Dbf4 phosphorylation. *Genes Dev.* 23:643–654. doi:10.1101/gad.1759609

Ge, X.Q., and J.J. Blow. 2009. The licensing checkpoint opens up. *Cell Cycle.* 8:2320–2322.

Ge, X.Q., D.A. Jackson, and J.J. Blow. 2007. Dormant origins licensed by excess Mcm2-7 are required for human cells to survive replicative stress. *Genes Dev.* 21:3331–3341. doi:10.1101/gad.457807

Gerlich, D., B. Koch, F. Dupeux, J.M. Peters, and J. Ellenberg. 2006. Live-cell imaging reveals a stable cohesin-chromatin interaction after but not before DNA replication. *Curr. Biol.* 16:1571–1578. doi:10.1016/j.cub.2006.06.068

Gilbert, D.M. 2007. Replication origin plasticity, Taylor-made: inhibition vs recruitment of origins under conditions of replication stress. *Chromosoma.* 116:341–347. doi:10.1007/s00412-007-0105-9

Görisch, S.M., A. Sporbert, J.H. Stear, I. Grunewald, D. Nowak, E. Warbrick, H. Leonhardt, and M.C. Cardoso. 2008. Uncoupling the replication machinery: replication fork progression in the absence of processive DNA synthesis. *Cell Cycle.* 7:1983–1990.

Hager, G.L., J.G. McNally, and T. Misteli. 2009. Transcription dynamics. *Mol. Cell.* 35:741–753. doi:10.1016/j.molcel.2009.09.005

Harada, H., H. Nakagawa, M. Takaoka, J. Lee, M. Herlyn, J.A. Diehl, and A.K. Rustgi. 2008. Cleavage of MCM2 licensing protein fosters senescence in human keratinocytes. *Cell Cycle.* 7:3534–3538.

Ibarra, A., E. Schwob, and J. Méndez. 2008. Excess MCM proteins protect human cells from replicative stress by licensing backup origins of replication. *Proc. Natl. Acad. Sci. USA.* 105:8956–8961. doi:10.1073/pnas.0803978105

Ilves, I., T. Petojevic, J.J. Pesavento, and M.R. Botchan. 2010. Activation of the MCM2-7 helicase by association with Cdc45 and GINS proteins. *Mol. Cell.* 37:247–258. doi:10.1016/j.molcel.2009.12.030

Izumi, M., and D.M. Gilbert. 1999. Homogeneous tetracycline-regulatable gene expression in mammalian fibroblasts. *J. Cell. Biochem.* 76:280–289. doi:10.1002/(SICI)1097-4644(20000201)76:2<280::AID-JCB11>3.0.CO;2-0

Keezer, S.M., and D.M. Gilbert. 2002. Sensitivity of the origin decision point to specific inhibitors of cellular signaling and metabolism. *Exp. Cell Res.* 273:54–64. doi:10.1006/excr.2001.5421

Kimura, H., and P.R. Cook. 2001. Kinetics of core histones in living human cells: little exchange of H3 and H4 and some rapid exchange of H2B. *J. Cell Biol.* 153:1341–1353. doi:10.1083/jcb.153.7.1341

Kimura, H., T. Ohtomo, M. Yamaguchi, A. Ishii, and K. Sugimoto. 1996. Mouse MCM proteins: complex formation and transportation to the nucleus. *Genes Cells.* 1:977–993. doi:10.1046/j.1365-2443.1996.840284.x

Komamura-Kohno, Y., K. Karasawa-Shimizu, T. Saitoh, M. Sato, F. Hanaoka, S. Tanaka, and Y. Ishimi. 2006. Site-specific phosphorylation of MCM4 during the cell cycle in mammalian cells. *FEBS J.* 273:1224–1239. doi:10.1111/j.1742-4658.2006.05146.x

Krude, T., C. Musahl, R.A. Laskey, and R. Knippers. 1996. Human replication proteins hCdc21, hCdc46 and P1Mcm3 bind chromatin uniformly before S-phase and are displaced locally during DNA replication. *J. Cell Sci.* 109:309–318.

Leonhardt, H., H.P. Rahn, P. Weinzierl, A. Sporbert, T. Cremer, D. Zink, and M.C. Cardoso. 2000. Dynamics of DNA replication factories in living cells. *J. Cell Biol.* 149:271–280. doi:10.1083/jcb.149.2.271

Liu, P., D.M. Slater, M. Lenburg, K. Nevis, J.G. Cook, and C. Vaziri. 2009. Replication licensing promotes cyclin D1 expression and G1 progression in untransformed human cells. *Cell Cycle.* 8:125–136.

Manser, T., T. Thacher, and M. Rechsteiner. 1980. Arginine-rich histones do not exchange between human and mouse chromosomes in hybrid cells. *Cell.* 19:993–1003. doi:10.1016/0092-8674(80)90090-2

Masai, H., C. Taniyama, K. Ogino, E. Matsui, N. Kakusho, S. Matsumoto, J.M. Kim, A. Ishii, T. Tanaka, T. Kobayashi, et al. 2006. Phosphorylation of MCM4 by Cdc7 kinase facilitates its interaction with Cdc45 on the chromatin. *J. Biol. Chem.* 281:39249–39261. doi:10.1074/jbc.M608935200

Masai, H., S. Matsumoto, Z. You, N. Yoshizawa-Sugata, and M. Oda. 2010. Eukaryotic chromosome DNA replication: where, when, and how? *Annu. Rev. Biochem.* 79:89–130. doi:10.1146/annurev.biochem.052308.103205

McNairn, A.J., Y. Okuno, T. Misteli, and D.M. Gilbert. 2005. Chinese hamster ORC subunits dynamically associate with chromatin throughout the cell-cycle. *Exp. Cell Res.* 308:345–356. doi:10.1016/j.yexcr.2005.05.009

Méndez, J., and B. Stillman. 2000. Chromatin association of human origin recognition complex, cdc6, and minichromosome maintenance proteins during the cell cycle: assembly of prereplication complexes in late mitosis. *Mol. Cell. Biol.* 20:8602–8612. doi:10.1128/MCB.20.22.8602-8612.2000

Misteli, T. 2001. Protein dynamics: implications for nuclear architecture and gene expression. *Science.* 291:843–847. doi:10.1126/science.291.5505.843

Mueller, F., D. Mazza, T.J. Stasevich, and J.G. McNally. 2010. FRAP and kinetic modeling in the analysis of nuclear protein dynamics: what do we really know? *Curr. Opin. Cell Biol.* 22:403–411. doi:10.1016/j.ceb.2010.03.002

Nevis, K.R., M. Cordeiro-Stone, and J.G. Cook. 2009. Origin licensing and p53 status regulate Cdk2 activity during G(1). *Cell Cycle.* 8:1952–1963.

O'Keefe, R.T., S.C. Henderson, and D.L. Spector. 1992. Dynamic organization of DNA replication in mammalian cell nuclei: spatially and temporally defined replication of chromosome-specific alpha-satellite DNA sequences. *J. Cell Biol.* 116:1095–1110. doi:10.1083/jcb.116.5.1095

Okuno, Y., A.J. McNairn, N. den Elzen, J. Pines, and D.M. Gilbert. 2001. Stability, chromatin association and functional activity of mammalian pre-replication complex proteins during the cell cycle. *EMBO J.* 20:4263–4277. doi:10.1093/emboj/20.15.4263

Pasero, P., B.P. Duncker, E. Schwob, and S.M. Gasser. 1999. A role for the Cdc7 kinase regulatory subunit Dbf4p in the formation of initiation-competent origins of replication. *Genes Dev.* 13:2159–2176. doi:10.1101/gad.13.16.2159

Pereverzeva, I., E. Whitmire, B. Khan, and M. Coué. 2000. Distinct phosphoisoforms of the *Xenopus* Mcm4 protein regulate the function of the Mcm complex. *Mol. Cell. Biol.* 20:3667–3676. doi:10.1128/MCB.20.10.3667-3676.2000

Phair, R.D., and T. Misteli. 2000. High mobility of proteins in the mammalian cell nucleus. *Nature.* 404:604–609. doi:10.1038/35007077

Phair, R.D., P. Scaffidi, C. Elbi, J. Vecerová, A. Dey, K. Ozato, D.T. Brown, G. Hager, M. Bustin, and T. Misteli. 2004. Global nature of dynamic protein-chromatin interactions in vivo: three-dimensional genome scanning and dynamic interaction networks of chromatin proteins. *Mol. Cell. Biol.* 24:6393–6402. doi:10.1128/MCB.24.14.6393-6402.2004

Philimonenko, A.A., D.A. Jackson, Z. Hodný, J. Janácek, P.R. Cook, and P. Hozák. 2004. Dynamics of DNA replication: an ultrastructural study. *J. Struct. Biol.* 148:279–289. doi:10.1016/j.jsb.2004.08.001

Remus, D., and J.F. Diffley. 2009. Eukaryotic DNA replication control: lock and load, then fire. *Curr. Opin. Cell Biol.* 21:771–777. doi:10.1016/j.ceb.2009.08.002

Remus, D., F. Beuron, G. Tolun, J.D. Griffith, E.P. Morris, and J.F. Diffley. 2009. Concerted loading of Mcm2-7 double hexamers around DNA during DNA replication origin licensing. *Cell.* 139:719–730. doi:10.1016/j.cell.2009.10.015

Romanowski, P., M.A. Madine, and R.A. Laskey. 1996. XMCM7, a novel member of the *Xenopus* MCM family, interacts with XMCM3 and colocalizes with it throughout replication. *Proc. Natl. Acad. Sci. USA.* 93:10189–10194. doi:10.1073/pnas.93.19.10189

Rothbauer, U., K. Zolghadr, S. Muyldermans, A. Schepers, M.C. Cardoso, and H. Leonhardt. 2008. A versatile nanotrap for biochemical and functional studies with fluorescent fusion proteins. *Mol. Cell. Proteomics.* 7:282–289.

Rowles, A., S. Tada, and J.J. Blow. 1999. Changes in association of the *Xenopus* origin recognition complex with chromatin on licensing of replication origins. *J. Cell Sci.* 112:2011–2018.

Sasaki, T., S. Ramanathan, Y. Okuno, C. Kumagai, S.S. Shaikh, and D.M. Gilbert. 2006. The Chinese hamster dihydrofolate reductase replication origin decision point follows activation of transcription and suppresses initiation of replication within transcription units. *Mol. Cell. Biol.* 26:1051–1062. doi:10.1128/MCB.26.3.1051-1062.2006

Shaner, N.C., G.H. Patterson, and M.W. Davidson. 2007. Advances in fluorescent protein technology. *J. Cell Sci.* 120:4247–4260. doi:10.1242/jcs.005801

Sheu, Y.J., and B. Stillman. 2010. The Dbf4-Cdc7 kinase promotes S phase by alleviating an inhibitory activity in Mcm4. *Nature.* 463:113–117. doi:10.1038/nature08647

Snyder, M., W. He, and J.J. Zhang. 2005. The DNA replication factor MCM5 is essential for Stat1-mediated transcriptional activation. *Proc. Natl. Acad. Sci. USA.* 102:14539–14544. doi:10.1073/pnas.0507479102

Stasevich, T.J., F. Mueller, D.T. Brown, and J.G. McNally. 2010. Dissecting the binding mechanism of the linker histone in live cells: an integrated FRAP analysis. *EMBO J.* 29:1225–1234. doi:10.1038/emboj.2010.24

Stoeber, K., T.D. Tlsty, L. Happerfield, G.A. Thomas, S. Romanov, L. Bobrow, E.D. Williams, and G.H. Williams. 2001. DNA replication licensing and human cell proliferation. *J. Cell Sci.* 114:2027–2041.

Todorov, I.T., A. Attaran, and S.E. Kearsey. 1995. BM28, a human member of the MCM2-3-5 family, is displaced from chromatin during DNA replication. *J. Cell Biol.* 129:1433–1445. doi:10.1083/jcb.129.6.1433

Tsakraklides, V., and S.P. Bell. 2010. Dynamics of pre-replicative complex assembly. *J. Biol. Chem.* 285:9437–9443. doi:10.1074/jbc.M109.072504

Wei, Z., C. Liu, X. Wu, N. Xu, B. Zhou, C. Liang, and G. Zhu. 2010. Characterization and structure determination of the Cdt1 binding domain of human minichromosome maintenance (Mcm) 6. *J. Biol. Chem.* 285:12469–12473. doi:10.1074/jbc.C109.094599

Wu, J.R., and D.M. Gilbert. 1996. A distinct G1 step required to specify the Chinese hamster DHFR replication origin. *Science.* 271:1270–1272. doi:10.1126/science.271.5253.1270

Wu, J.R., and D.M. Gilbert. 1997. The replication origin decision point is a mitogen-independent, 2-aminopurine-sensitive, G1-phase event that precedes restriction point control. *Mol. Cell. Biol.* 17:4312–4321.

Xouri, G., A. Squire, M. Dimaki, B. Geverts, P.J. Verveer, S. Taraviras, H. Nishitani, A.B. Houtsmuller, P.I. Bastiaens, and Z. Lygerou. 2007. Cdt1 associates dynamically with chromatin throughout G1 and recruits Geminin onto chromatin. *EMBO J.* 26:1303–1314. doi:10.1038/sj.emboj.7601597

Yankulov, K., I. Todorov, P. Romanowski, D. Licatalosi, K. Cilli, S. McCracken, R. Laskey, and D.L. Bentley. 1999. MCM proteins are associated with RNA polymerase II holoenzyme. *Mol. Cell. Biol.* 19:6154–6163.

Zhang, J.J., Y. Zhao, B.T. Chait, W.W. Lathem, M. Ritzi, R. Knippers, and J.E. Darnell Jr. 1998. Ser727-dependent recruitment of MCM5 by Stat1alpha in IFN-gamma-induced transcriptional activation. *EMBO J.* 17:6963–6971. doi:10.1093/emboj/17.23.6963